Stable, Cationic Alkyl−Olefin Complexes of Ruthenium(II) and Rhodium(III): Effects of Ligand Geometry upon Olefin Insertion/Alkyl Migration

Eric L. Dias, Maurice Brookhart,* and Peter S. White

Department of Chemistry, University of North Carolina at Chapel Hill, Chapel Hill, North Carolina 27599-3290

Received August 4, 2000

The syntheses of ruthenium(II) and rhodium(III) model complexes of the putative active species in the iron(II)/MMAO polymerization system are reported. The cationic ruthenium methyl ethylene complex **3** is a stable, isolable compound, which does not produce polyethylene under a variety of conditions. Likewise, the analogous rhodium complex **12** shows no appreciable polymerization activity, despite its similarity to existing rhodium complexes which are active catalysts for olefin polymerization. X-ray crystal structures of the cationic ruthenium bis(ethylene) complex **7** and the five-coordinate rhodium bis(triflate) methyl complex **9** are also presented.

Introduction

Following the discovery that transition-metal complexes could catalyze the polymerization of ethylene and α-olefins, a considerable amount of effort has been dedicated to the design of new catalyst systems.[1] By varying the catalyst structure, the molecular weight, composition, and tacticity of the resulting polymers can be altered, allowing the properties of the material to be controlled.[1c−h] While the majority of catalysts are based on early transition metals, the advent of the nickel and palladium diimine catalysts,[2] which can produce polyethylene with various degrees of branching depending on the polymerization conditions,[2b,h] has sparked a great deal of interest in late-transition-metal catalysts as well.[1a,b]

Recently, it was reported by Bennett at DuPont,[3a,b] our group,[3c] and Gibson's group[4] that the 2,6-diketiminoylpyridine complexes of iron(II) dihalides **1** are effective precursors for the polymerization of ethylene to either oligomers[5] or high molecular weight polymer,[3,4] depending upon the steric bulk of the ligand employed (eq 1). Upon treatment with modified methylaluminoxane (MMAO), exceptionally active catalysts are produced, consuming ethylene at rates of up to 10^6 turnovers/h.[3−5] The polymers produced in this manner, however, often exhibit multimodal polydispersities, which can drastically affect the mechanical properties of the materials. In addition, the high activities of the catalysts along with the required excess cocatalyst (MAO or MMAO) make this an increasingly difficult system to study.

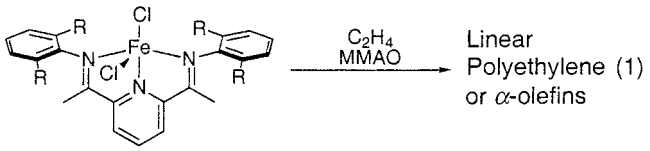

1

By analogy with several well-defined olefin polymerization catalysts,[1] the putative active species in this system is believed to be the cationic iron alkyl complex **2**, which may have a molecule of ethylene bound under the polymerization conditions. Although theoretical studies using cationic iron(II) alkyl model compounds have been performed,[6] experimental evidence for the

(1) For reviews of organometallic catalysis in olefin polymerization, see: (a) Ittel, S. D.; Johnson, L. K.; Brookhart, M. *Chem. Rev.* **2000**, *100*, 1169−1203. (b) Britovsek, G. J. P.; Gibson, V. C.; Wass, D. F. *Angew. Chem., Int. Ed.* **1999**, *38*, 428−447. (c) Kaminsky, W. *J. Chem. Soc., Dalton Trans.* **1998**, 1413−1418. (d) Soga, K.; Shiono, T. *Prog. Polym. Sci.* **1997**, *22*, 1503−1546. (e) Bochmann, M. *J. Chem. Soc., Dalton Trans.* **1996**, 255−270. (f) Brintzinger, H. H.; Fischer, D.; Mulhaupt, R.; Rieger, B.; Waymouth, R. M. *Angew. Chem., Int. Ed. Engl.* **1995**, *34*, 1143−1170. (g) Mohring, P. C.; Coville, N. J. *J. Organomet. Chem.* **1994**, *479*, 1−29. (h) Gupta, V. K.; Satish, S.; Bhardwaj, I. S. *Rev. Macromol. Chem. Phys. C* **1994**, *34*, 439−514.

(2) (a) Svejda, S. A.; Johnson, L. K.; Brookhart, M. *J. Am. Chem. Soc.* **1999**, *121*, 10634−10635. (b) Guan, Z. B.; Cotts, P. M.; McCord, E. F.; McLain, S. J. *Science* **1999**, *283*, 2059−2062. (c) McLain, S. J.; Feldman, J.; McCord, E. F.; Gardner, K. H.; Teasley, M. F.; et al. *Macromolecules* **1998**, *31*, 6705−6707. (d) Mecking, S.; Johnson, L. K.; Wang, L.; Brookhart, M. *J. Am. Chem. Soc.* **1998**, *120*, 888−899. (e) Killian, C. M.; Johnson, L. K.; Brookhart, M. *Organometallics* **1997**, *16*, 2005−2007. (f) Killian, C. M.; Tempel, D. J.; Johnson, L. K.; Brookhart, M. *J. Am. Chem. Soc.* **1996**, *118*, 11664−11665. (g) Johnson, L. K.; Mecking, S.; Brookhart, M. *J. Am. Chem. Soc.* **1996**, *118*, 267−268. (h) Johnson, L. K.; Killian, C. M.; Brookhart, M. *J. Am. Chem. Soc.* **1995**, *117*, 6414−6415.

(3) (a) Bennett, A. M. A. WO9827124 to DuPont. (b) Bennett, A. M. A. *CHEMTECH* **1999**, *29*, 24. (c) Small, B. L.; Brookhart, M.; Bennett, A. M. A. *J. Am. Chem. Soc.* **1998**, *120*, 4049−4050.

(4) (a) Britovsek, G. J. P.; Bruce, M.; Gibson, V. C.; Kimberley, B. S.; Maddox, P. J.; Mastroianni, S.; et al. *J. Am. Chem. Soc.* **1999**, *121*, 8728−8740. (b) Britovsek, G. J. P.; Gibson, V. C.; Kimberley, B. S.; Maddox, P. J.; McTavish, S. J.; et al. *Chem. Commun.* **1998**, 849−850.

(5) Small, B. L.; Brookhart, M. *J. Am. Chem. Soc.* **1998**, *120*, 7143−7144.

(6) (a) Deng, L. Q.; Margl, P.; Ziegler, T. *J. Am. Chem. Soc.* **1999**, *121*, 6479−6487. (b) Griffiths, E. A. H.; Britovsek, G. J. P.; Gibson, V. C.; Gould, I. R. *Chem. Commun.* **1999**, 1333−1334.

10.1021/om000674i CCC: $19.00
Publication on Web 10/21/2000

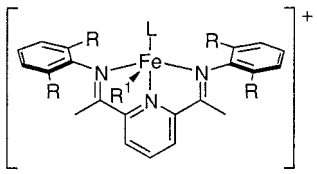

2

stability and reactivity of species such as **2** is still somewhat lacking. To understand this system in further detail, we chose to synthesize the analogous ruthenium(II) complex, which is expected to exhibit polymerization activity lower than that of the iron system without the need for a cocatalyst or activator, making it more amenable to study.

In this paper, we report the synthesis and isolation of the *stable*, cationic ruthenium methyl ethylene complex **3** and the corresponding carbon monoxide adduct **4**. Neither of these complexes are effective initiators for

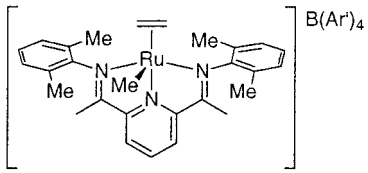

3

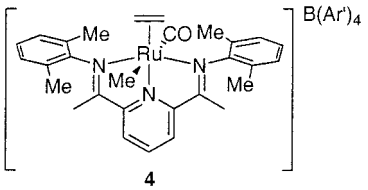

4

the polymerization of ethylene and α-olefins or the copolymerization of olefins and CO. The synthesis of an analogous isoelectronic, dicationic rhodium methyl ethylene complex, which behaves in a similar fashion, is also presented. Because the nickel and palladium diimine complexes both act as initiators for olefin polymerization, reasons for this apparent break in the periodic trend will be discussed.

Results and Discussion

Synthesis of the Cationic Ruthenium Methyl Ethylene Complexes 3 and 4. The ruthenium complex **3** was synthesized in three steps, starting from [(*p*-cymene)$RuCl_2$]$_2$.[7] Refluxing a solution of the 2,6-diketiminoylpyridine ligand **5a**[3] and [(*p*-cymene)$RuCl_2$]$_2$ in ethanol[8] under an ethylene atmosphere produces, upon cooling, the ethylene complex **6** as a purple, microcrystalline solid in 85% yield (eq 2). It should be noted, however, that this reaction does *not* work when the substituents in the *ortho* positions are too bulky. For instance, if the ligand **5b** derived from 2,6-diisopropylaniline is used instead of **5a**, no reaction is observed. Several attempts were made to synthesize complexes of **5b** from a wide variety of ruthenium precursors, with little success.

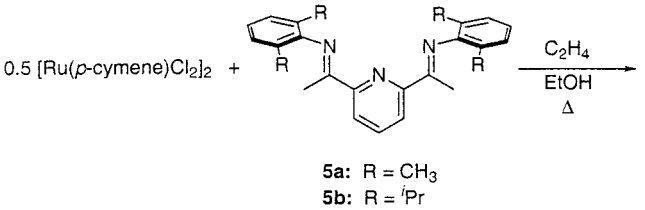

5a: R = CH_3
5b: R = ^{i}Pr

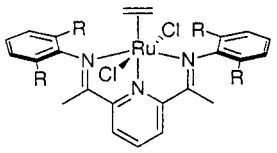

6: R = CH_3 (2)

Direct alkylation of **6** with MeLi, MeMgBr, or $MgMe_2$ gave inconsistent results at best, even under strict temperature control. While reaction of MeLi in THF did in one case produce what appeared to be an alkylated complex, this was not reproducible to a satisfactory degree. As a result, we chose to form a cationic ruthenium complex *prior* to alkylation.

Reaction of **6** with 1 equiv of $NaB(Ar')_4$ (Ar′ = 3,5-bis(trifluoromethyl)phenyl) under an ethylene atmosphere in dichloromethane produces the bis(ethylene) complex **7** (eq 3). The reaction is surprisingly clean, and

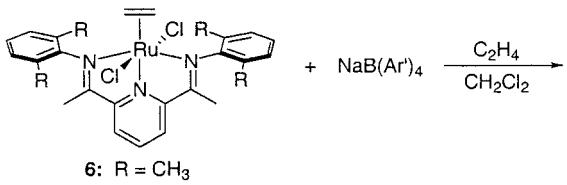

6: R = CH_3

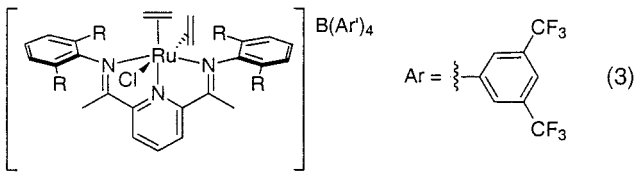

7: R = CH_3 (3)

after recrystallization from dichloromethane/pentane (ca. 1/1 v/v) the product is obtained as a stable, dark red crystalline solid. Both ethylene molecules remain bound after drying *in vacuo* overnight.

The crystal structure of **7** reveals many details about the ruthenium complex with this particular ligand that otherwise would not have been apparent (Figure 1). The geometry of **7** is best described as a distorted octahedron. Using the nitrogen atoms N(5), N(13), and N(24) along with the central ruthenium atom to define the equatorial plane of the complex, the N(5)−Ru−Cl angle of 82° indicates significant deviation from the expected 90° angle (Table 2). The ethylene molecules are also bound in a nonstandard coordination geometry. Using the centroid of C(1) and C(2), the N(5)−Ru−(C−C) angle is 95.2°, and likewise the N(5)−Ru−(C−C) angle for C(3) and C(4) is 167°—a deviation of 13° from the equatorial plane! It is immediately apparent from space-filling models that the *o*-methyl substituents on the ligand aryl groups are at least in part responsible for the atypical geometry, as the Ru−Cl bond length places the chlorine atom directly in the most sterically demanding region

(7) Bennett, M. A.; Huang, T.-N.; Matheson, T. W.; Smith, A. K. *Inorg. Synth.* **1982**, *21*, 75.
(8) (a) Cetinkaya, B.; Cetinkaya, E.; Brookhart, M.; White, P. S. *J. Mol. Catal. A* **1999**, *142*, 101−112. (b) Bianchini, C.; Lee, H. M. *Organometallics* **2000**, *19*, 1833−1840.

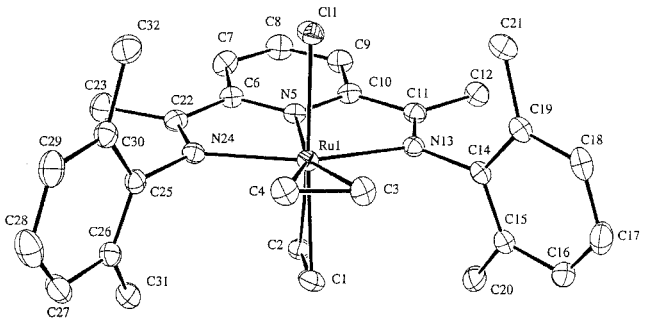

Figure 1. X-ray crystal structure of **7**. Thermal ellipsoids are drawn at the 50% probability level.

Table 1. Summary of Crystallographic Data for 7 and 9

	7	**9**
formula	$BClC_{61}F_{24}H_{47}N_3Ru$	$C_{36}F_6H_{46}N_3O_6RhS_2$
mol wt	1425.35	897.81
color	red	orange
cryst syst	triclinic	orthorhombic
space group	*P*1	*Pcab*
a (Å)	10.0974(6)	16.1396(10)
b (Å)	16.7117(10)	22.7895(15)
c (Å)	18.8344(12)	25.2719(16)
α (deg)	105.224(1)	90
β (deg)	91.486(1)	90
γ (deg)	97.609(1)	90
V (Å^3)	3033.5(3)	9295.3(10)
Z	2	8
D_{calcd} (Mg m^3)	1.560	1.389
wavelength (Å)	0.710 73	0.710 73
μ (mm^{-1})	0.42	0.53
cryst dimens (mm)	0.30 × 0.30 × 0.10	0.35 × 0.35 × 0.15
temp (°C)	−100	−100
mode	*ω*	*ω*
scan width (deg)	0.3	0.3
octants	±*h*,*k*,*l*	±*h*,*k*,*l*
$2\theta_{max}$ (deg)	50.0	50.0
no. of rflns	31 116	56 256
no. of unique rflns	10 727	8233
no. of data with $I > 2.5\sigma$	8797	6975
R(*F*)	0.050 (0.059)	0.039 (0.051)
R_w(*F*)	0.063 (0.065)	0.041 (0.046)
largest peak in final diff map (e Å^{-3})	1.350	2.960
GOF	2.90	5.37

Table 2. Selected Distances and Angles for 7

Distances (Å)			
Ru(1)−C(2)	2.229(4)	Ru(1)−N(24)	2.140(3)
Ru(1)−C(3)	2.265(4)	Ru(1)−Cl(1)	2.4060(11)
Ru(1)−N(5)	1.992(3)		

Angles (deg)			
N(5)−Ru(1)−Cl(1)	81.60(10)	N(5)−Ru(1)−c[C(1)C(2)]	95
N(5)−Ru(1)−N(24)	77.40(13)	N(5)−Ru(1)−c[C(3)C(4)]	167

of the ligand. In fact, the distance between the chlorine atom and the methyl groups is shorter than the sum of their respective van der Waals radii, explaining the difficulty encountered when using ligand **5b**, which contains much bulkier isopropyl substituents.

A 2D ^{1}H NOESY measurement, which was acquired to provide a complete assignment of the peaks in the 1D ^{1}H NMR spectrum, provides evidence that this geometry is also present in solution (Figure 2), ruling out distortions due to crystal-packing forces. While the ethylene molecule bound in the axial position (3.3 ppm) displays a very strong NOE to the aryl−methyl groups at 1.7 ppm as expected, the ethylene molecule bound in the equatorial position (4.4 ppm) displays only a very weak NOE to these methyl groups and a strong NOE to the *other* aryl−methyl groups at 2.2 ppm, consistent with the distorted geometry observed in the crystal structure.

Alkylation of **7** was effected in dichloromethane using (tmeda)$MgMe_2$,[9] favored due to its solubility in noncoordinating solvents which are incapable of displacing ethylene from the complex. Isolation of the crude product, however, indicated that there was an equilibrium between the cationic ruthenium methyl ethylene complex **3** and the ruthenium methyl ethylene chloro complex (eq 4). To drive the equilibrium completely to

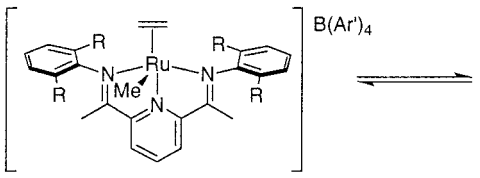

3: R = CH_3

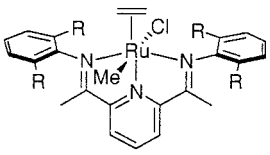

(4)

3, addition of 1 equiv of $NaB(Ar')_4$ was required (eq 5). After evaporation of the solvent *in vacuo*, the product **3** was extracted from the magnesium salts at −78 °C, with a solvent mixture of 1/4 v/v dichloromethane/pentane. Upon removal of the solvent at room temperature, the product is obtained as a brittle, dark green foam, in relatively low yield (25%). Alternatively, the product can be purified by column chromatography (Florisil) under an inert atmosphere, generally giving much higher yields (73%).

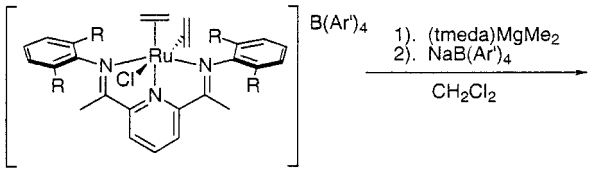

7: R = CH_3

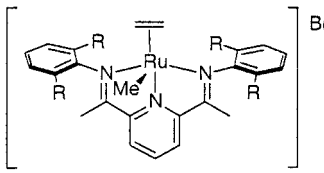

(5)

3: R = CH_3

Because the product tends to form an intractable oily residue when exposed to solvents other than dichloromethane, attempts to crystallize **3** have been unsuccessful to date. The complex was therefore characterized by NMR spectroscopy (Figure 3). As expected, the ruthenium−methyl (1) resonance appears upfield at −1.01 ppm in the ^{1}H NMR spectrum. Two distinct

(9) Graser, T.; Kopf, J.; Thoennes, D.; Weiss, E. *J. Organomet. Chem.* **1980**, *191*, 1−6.

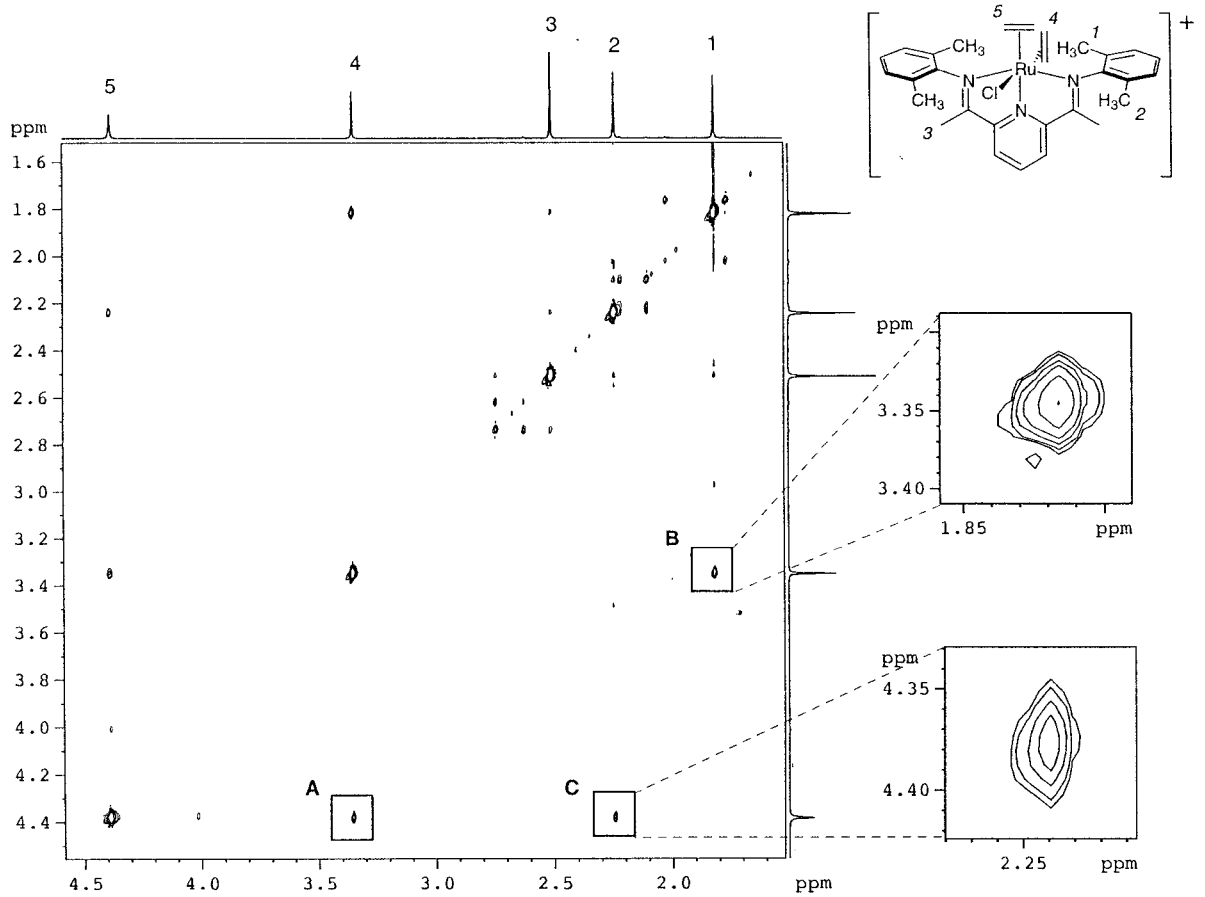

Figure 2. ^{1}H NOESY of **7** acquired at room temperature in CD_2Cl_2. Significant cross-peaks: (**A**) ethylene (4)−ethylene (5); (**B**) methyl (1)−ethylene (4); (**C**) methyl (2)−ethylene (5). The larger intensity of **B** compared to that of **C** provides an assignment of the respective ethylene and methyl resonances. The very weak cross-peak from methyl (1)−ethylene (5) is not shown for clarity.

resonances for the aryl−methyl groups (2, 3) are observed at 1.38 and 1.95 ppm, and a single, bound ethylene molecule (5) appears at 3.43 ppm. A 2D ^{1}H NOESY was also collected to establish that the complex actually possesses the depicted square-pyramidal geometry (Figure 4). It is readily apparent that there is a strong NOE between the ruthenium−methyl group (1) and the bound ethylene (5), indicating that they are in a *cis* arrangement. The ruthenium−methyl group (1) also displays a strong NOE to only one set of aryl−methyl resonances at 1.95 ppm (3), indicating that it is in an axial position. Finally, the bound ethylene (5) displays two cross-peaks of equal intensity to *both* aryl−methyl resonances (2, 3), providing conclusive evidence that it is bound in the equatorial position as illustrated.

Because complex **3** is five-coordinate, it might be expected that steric congestion around the Ru−methyl group could be relieved if the aryl groups were canted, *i.e.* not perpendicular to the plane of the ligand backbone, as depicted in Scheme 1. Rotation about the N−C(ipso) bonds in the complex has the net result of placing the aryl−methyl substituents (3) *closer* to, and the aryl−methyl groups (2) *further* from, the ketimine methyl groups (4) of the ligand backbone. Evidence for this behavior is provided by the magnitudes of the respective cross-peaks—the NOE between the backbone methyl groups (4) and the aryl−methyl groups (3) is noticably stronger than that for the methyl groups (2) (Figure 4).

The CO complex **4** is easily obtained by addition of 1 equiv of CO *via* syringe to a solution of **3** under an inert atmosphere (eq 6). After 30 min, the solution changes color from dark green to orange, and upon evaporation of the solvent a brittle, dark orange foam is obtained (similar to **3**).

Complex **4** was easily verified to be a carbonyl complex by both the CO stretch in the IR spectrum at $\nu = 2003$ cm^{-1} (KBr) and the peak at 183.68 ppm in the ^{13}C NMR spectrum (CD_2Cl_2). As with complex **3**, **4** was also characterized by 2D ^{1}H NMR spectroscopy to unambiguously establish its stereochemistry (Figure 5).

Scheme 1

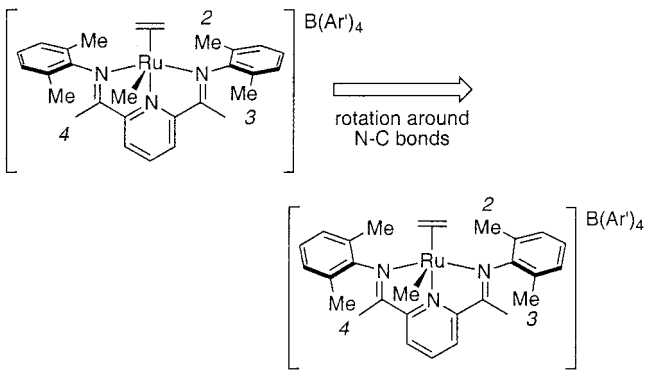

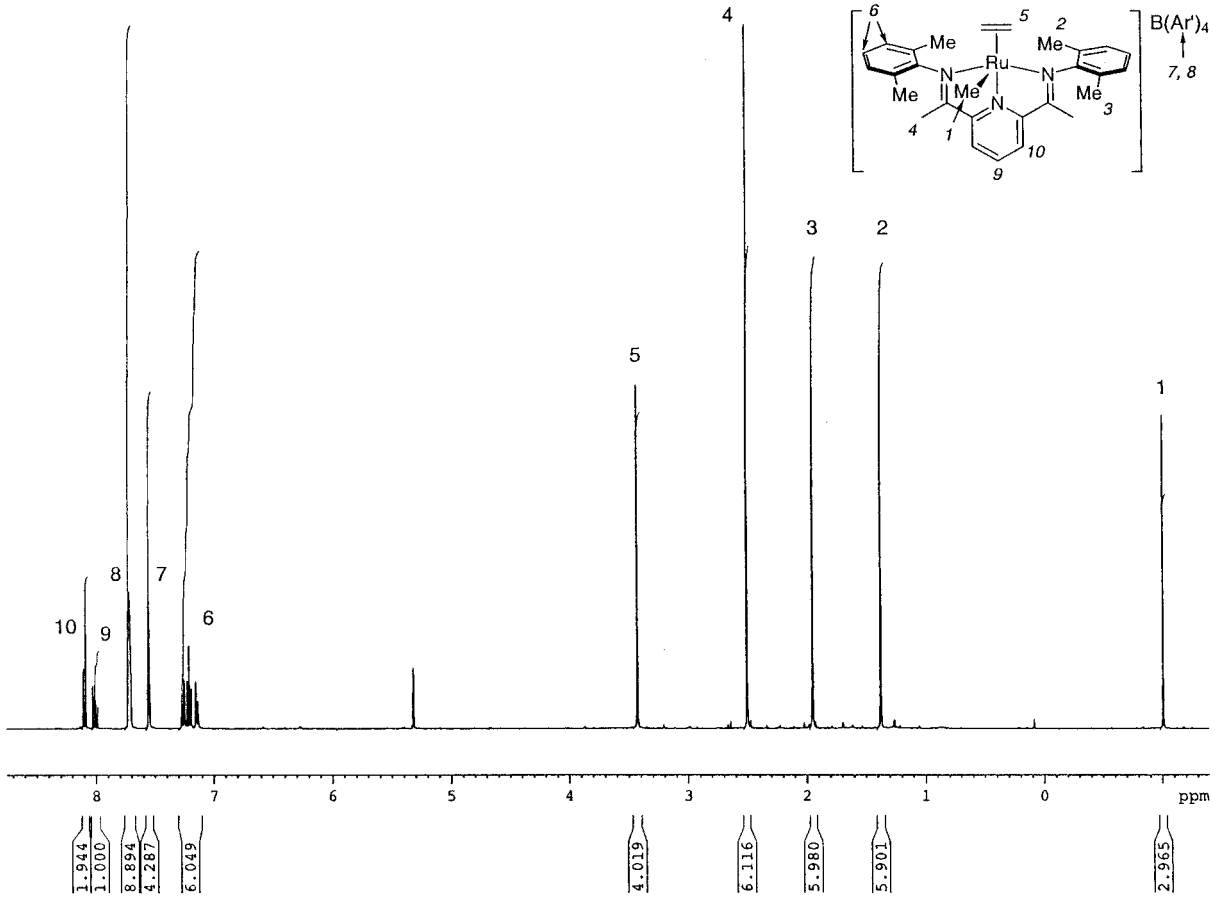

Figure 3. ^{1}H NMR spectrum of **3** in CD_2Cl_2. Peak assignments **2** and **3** are based on the 2D NOESY spectrum (Figure 4).

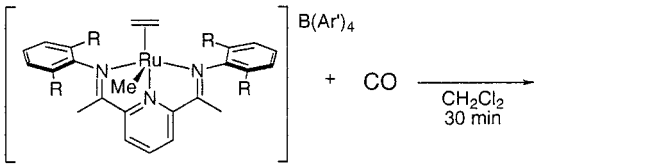

3: R = CH_3

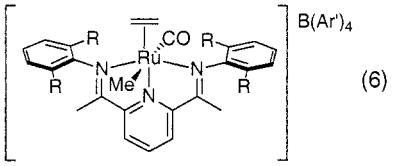

(6)

4: R = CH_3

The NOE between the methyl group and the bound ethylene is very strong, confirming their cis arrangement around the metal center. In addition, the NOE's between the ethylene and the aryl methyl groups do *not* have the same intensity, as was observed for **7**. Judging by the relative intensities of these cross-peaks, however, it can be concluded that while this complex is also a distorted octahedron, the deviations from ideal geometry are not as severe as with **7**.

Attempted Polymerizations Using 3. Because of the remarkable stability of **3** toward methyl migration to ethylene at room temperature, it was not expected that this complex would be a particularly active polymerization catalyst. When a dichloromethane solution of **3** is heated to 70 °C (in a closed system) under an ethylene atmosphere, however, there is still no apparent C−C bond formation. Even after the mixture is stirred for several hours under 400 psi of ethylene at room temperature, there is no evidence of either polymer or α-olefins. Extended heating at 80 °C in chlorobenzene, on the other hand, results in the very slow production of 1-butene. Because **3** is not stable at this temperature, the identity of the active species is not clear, given that butene production continues after all of the complex has apparently decomposed to unidentified products. Photolysis of a dichloromethane solution of **3** under an ethylene atmosphere only results in formation of the precursor complexes **6** and **7**. The use of other solvents is severely limited by the tendency of **3** to produce an intractable oil when exposed to nonpolar, nonchlorinated solvents. When using toluene or hexanes, however, there is still no polymer obtained.

Complex **3** was screened for activity in the copolymerization of ethylene/CO as well. Upon exposure of a dichloromethane solution of **3** to 1 atm of ethylene/CO, the color immediately changes from dark green to orange, and no polymer is obtained after extended periods of time. Presumably, the orange product is **4**, resulting from coordination of carbon monoxide to **3**.

Synthesis of Isoelectronic Rhodium(III) Complexes. Because of the surprising inactivity of **3** toward olefin polymerization, we also decided to explore its isolectronic rhodium(III) analogue. Because the rhodium(III) complex would be dicationic, it was expected to be more electrophilic and therefore more reactive than **3**. Given that Wang and Flood have demonstrated

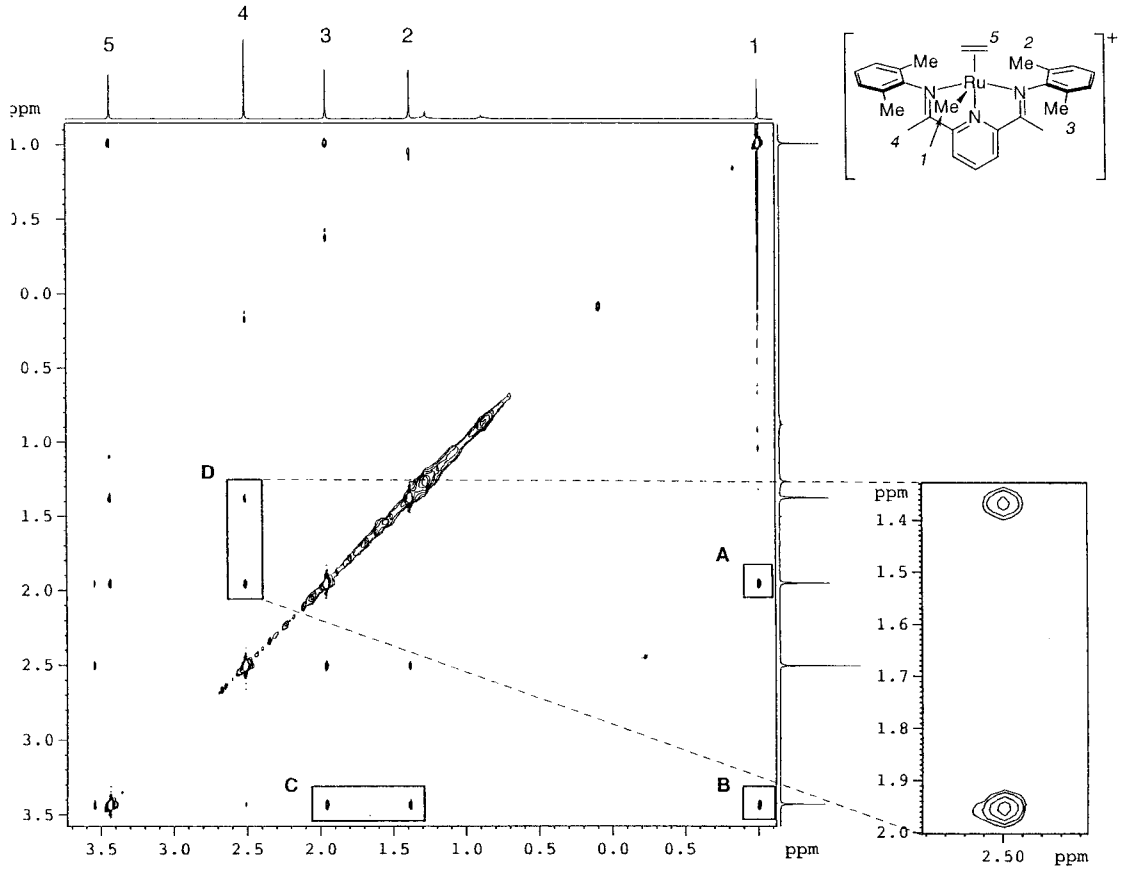

Figure 4. ^{1}H NOESY of **3** acquired at room temperature in CD_2Cl_2. Significant cross-peaks: (**A**) methyl (1)−methyl (3); (**B**) methyl (1)−ethylene (5); (**C**) ethylene (5)−methyl (2) and ethylene (5)−methyl (3); (**D**) methyl (4)−methyl (2) and methyl (4)−methyl (3). The difference in the relative intensities of cross-peaks **D** provide evidence for twisting of the aryl groups around the N−C(ipso) bonds (Scheme 1). The cross-peaks **C** (not enlarged) are of approximately equal intensity.

Table 3. Selected Distances and Angles for 9

Distances (Å)			
Rh(1)−C(7)	2.026(3)	Rh(1)−O(11)	2.0977(22)
Rh(1)−N(31)	1.911(3)	Rh(1)−O(21)	2.3578(21)
Rh(1)−N(5)	2.091(3)		

Angles (deg)			
C(7)−Rh(1)−N(31)	91.37(12)	C(4)−N(5)−C(61)−C(62)	−71.9(5)
N(5)−Rh(1)−N(31)	79.92(11)	C(1)−N(2)−C(41)−C(46)	76.0(5)

that the complexes (Cn)Rh(Me)$(X)_2$ (Cn = trimethyltriazacyclononane, X = OTf, BF_4) are effective initiators for the polymerization of ethylene,[10] the analogous rhodium complexes employing the 2,6-diketiminoylpyridine ligands **5** were attractive targets as polymerization initiators. The bis(triflate) complex **9** was readily synthesized in two steps from $[Rh(C_2H_4)_2Cl]_2$[11] via the compound [(**5b**)RhCl] (**8**), as shown in eq 7.[12]

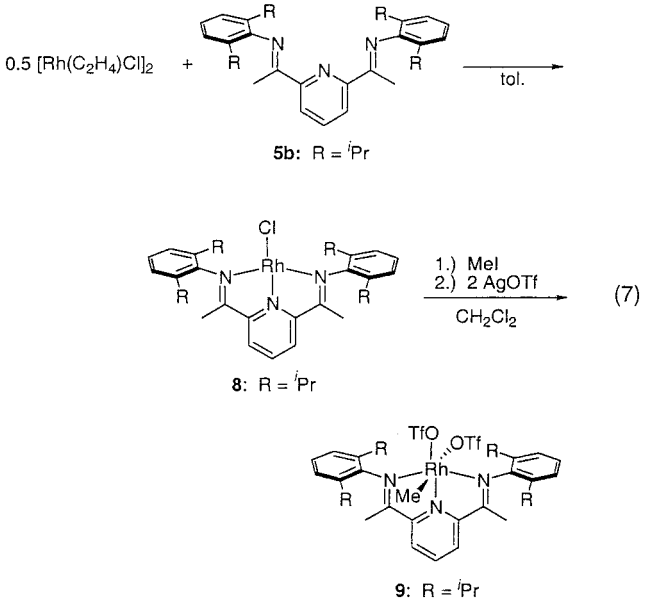

(7)

The crystal structure of **9** (Figure 6) reveals a few details worth noting. One significant feature is the difference between the Rh−O bond lengths for the two triflate groups. While the triflate bound cis to the methyl group has a normal Rh−O bond length of 2.098 Å (Table 3), the triflate that is bound trans to the methyl group has a very long Rh−O bond (2.358 Å). Because of the electronic *trans* influence of the methyl group in conjunction with the steric crowding imposed by the isopropyl groups, this triflate might better be described as a contact ion, with the rhodium metal center being five-coordinate. In accordance with this description, the aryl rings on the imines are twisted dramatically to accommodate the rhodium-bound methyl group, making the opposite site much less accessible—the same torsional configuration that is proposed for **3** on the basis of spectroscopic data.

(10) (a) Wang, L.; Lu, R. S.; Bau, R.; Flood, T. C. *J. Am. Chem. Soc.* **1993**, *115*, 6999−7000. (b) Wang, L.; Flood, T. C. *J. Am. Chem. Soc.* **1992**, *114*, 3169−3170.

(11) Cramer, R. *Inorg. Synth.* **1974**, *15*, 14−16.

(12) Haarmann, H. F.; Ernsting, J. M.; Kranenburg, M.; Kooijman, H.; Veldman, N.; et al. *Organometallics* **1997**, *16*, 887−900.

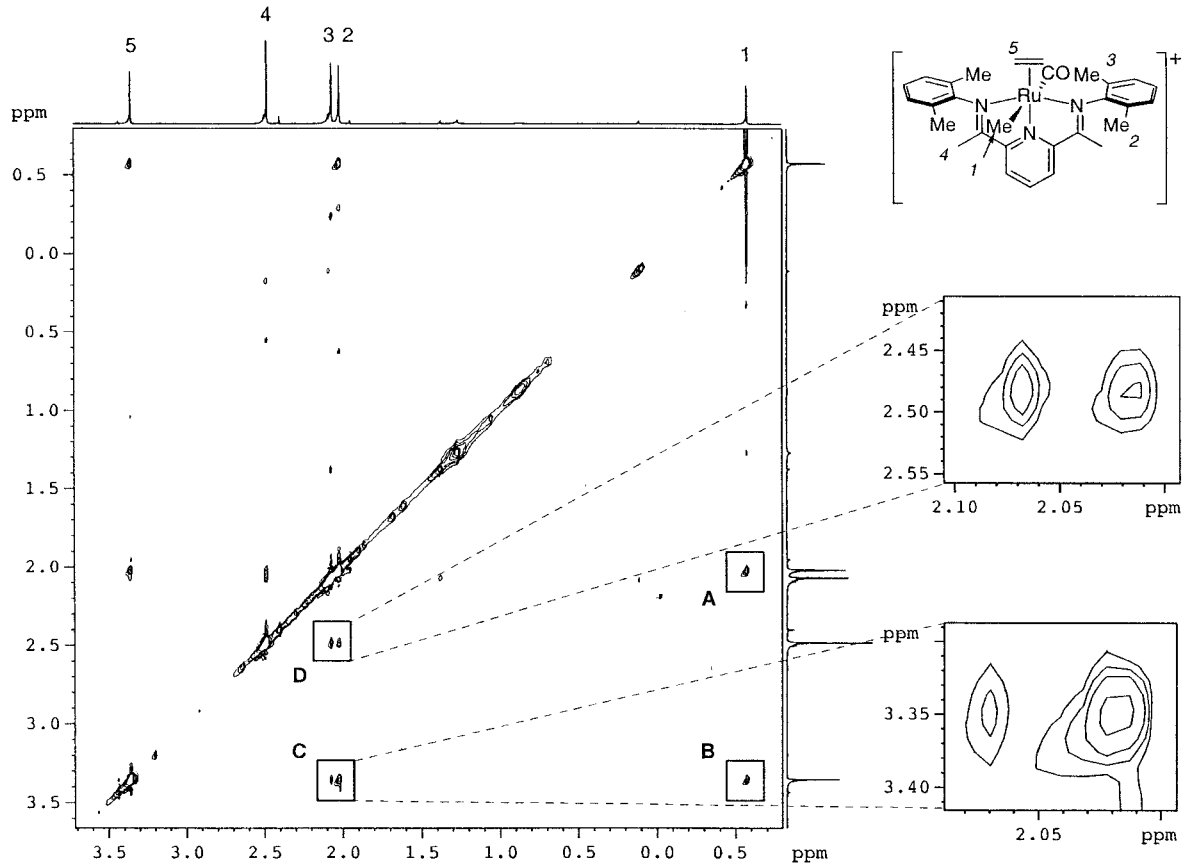

Figure 5. ^{1}H NOESY of **4** acquired at room temperature in CD_2Cl_2. Significant cross-peaks: (**A**) methyl (1)−methyl (2), (**B**) methyl (1)−ethylene (5); (**C**) ethylene (5)−methyl (2) and ethylene (5)−methyl (3); (**D**) methyl (4)−methyl (2) and methyl (4)−methyl (3). The difference in intensities of cross-peaks **C** indicate deviation from ideal octahedral geometry, as observed in **7**. The relatively equal intensities of cross-peaks **D** suggest that the aryl rings remain approximately perpendicular to the ligand backbone.

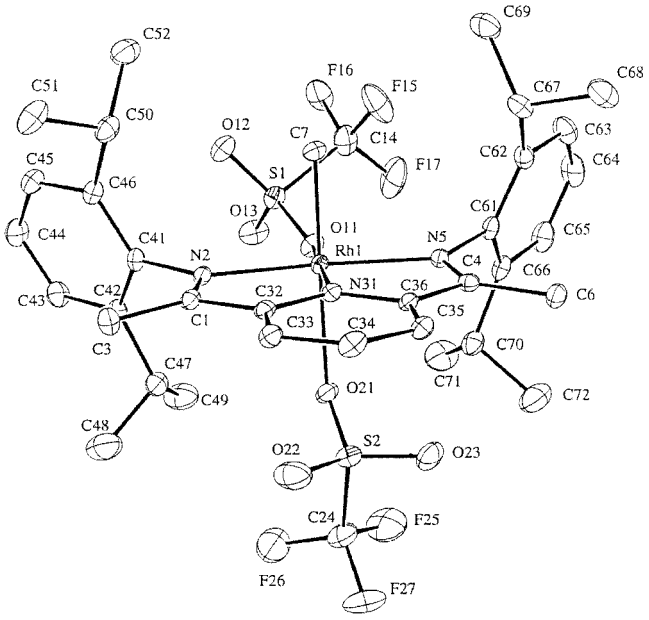

Figure 6. X-ray crystal structure of **9**. Thermal ellipsoids are drawn at the 50% probability level.

In contrast to what one would expect, reaction of **9** with Na(BAr′)$_4$ exchanges the triflate that is *cis* to the methyl group, as confirmed by a crystal structure of the corresponding aquo complex **13** (see the Supporting Information). Because of the problems encountered in exchanging the remaining triflate, a separate route was adopted for the synthesis of a dicationic, rhodium(III) methyl ethylene complex that would be isoelectronic and isostructural with the ruthenium complex **3**.

The first attempted route to a dicationic rhodium methyl ethylene complex is shown in eq 8. The cationic

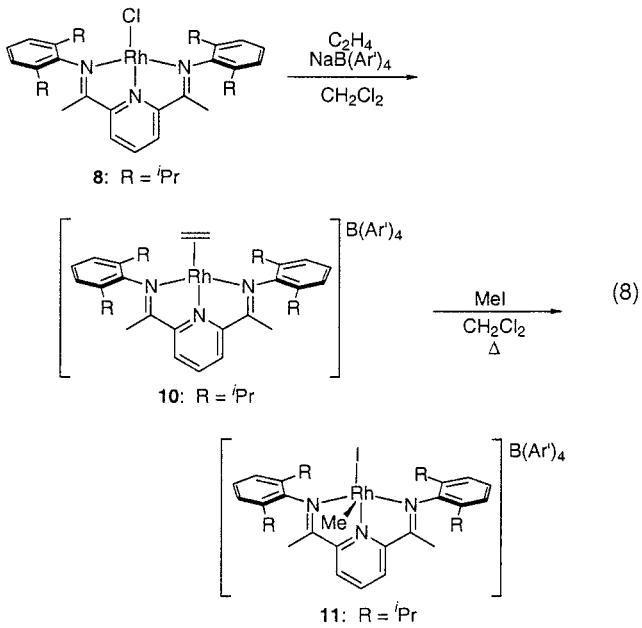

(8)

ethylene complex **10** is readily synthesized by the reaction of **8** with $NaB(Ar')_4$ under an ethylene atmosphere. Alkylation of **10** with methyl iodide could only be effected upon heating a dichloromethane solution to 45 °C for 4 h, during which time the color changes from orange to an intensely dark reddish pink. Upon removal of the solvent, the only product isolated is the five-coordinate complex **11**, in which the iodide has apparently displaced ethylene from the metal center. The crystal structure of **11** (Supporting Information) indicates that the methyl and iodide substituents are in a *cis* geometry, as expected, with the iodide trans to the pyridine moiety. In addition, the aryl rings are slightly canted to relieve steric congestion at the methyl-bound position, as is observed for both **3** and **9**.

The dicationic methyl ethylene complex **12**, containing two BF_4 anions, was finally obtained by the reaction of **11** with excess $AgBF_4$ under an ethylene atmosphere (eq 9). Complex **12** was not isolated as a pure solid,

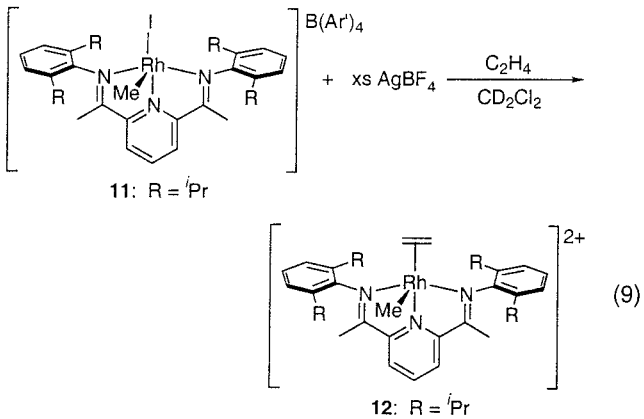

(9)

although it could be observed spectroscopically (Supporting Information).

Attempted Polymerizations using Rhodium Complexes 9 and 12. As with the ruthenium complexes, the triflate complex **9** does not produce polyethylene, or even butene, under conditions similar to those used for **7**. In the case of **12**, which was generated *in situ* under an ethylene atmosphere, no further reaction takes place, even after extended heating at 40 °C.

Conclusions

Although iron and ruthenium are both group VIII transition metals, it is immediately obvious that there are significant differences between them. The iron dichloride complexes of the ligands **5a** and **5b** are five-coordinate, possessing a square-pyramidal geometry in which the halides are in a *cis* configuration.[3,4] In the case of ruthenium, however, these complexes are always octahedral, with the halides in a *trans* geometry.[8] Electronically, the iron complexes are commonly high-spin,[3,4] while their ruthenium counterparts are inevitably low-spin. These are mainly empirical observations regarding these two systems, but they may have far-reaching effects regarding reactivity, as evidenced by the lack of polymerization activity for the ruthenium complex **3**.

The analogous rhodium complexes **9** and **12** provided even more of a surprise. Despite their overall similarity to the triazacylononane complexes studied by Flood *et al.*,[10] these systems once again do not exhibit any activity for the polymerization of ethylene. Because the ligand **5b** and triazacyclonane are expected to be fairly similar electronically, the difference *must* be due to the geometry imposed by the ligands—*i.e.*, *fac*-triazacyclononane versus *mer*-**5b**. The meridional geometry of these ligands necessarily differentiates the remaining binding sites around the metal center, creating distinct axial (*cis* to pyridine) and equatorial (*trans* to pyridine) positions—a feature that is lacking in both the diimine (Ni,Pd)[2] and triazacyclononane (Rh)[10] systems. By analogy, this may also be responsible for the inactivity observed with the ruthenium complex **3**. Experimentally, it has been observed that both the rhodium and ruthenium complexes are exceptionally stable with the alkyl and ethylene substituents in the axial and equatorial sites, respectively. Because migration of the methyl group to the ethylene is expected to form a species in which the newly formed metal−alkyl bond is in the equatorial position, the stability of such a species must now be considered as well.

In a separate paper, *ab initio* calculations of both the ruthenium and iron systems which support theseempirical conclusions will be presented.[13] The electronic nature of these ligands, in conjunction with the geometry of the intermediates, has unforeseen consequences upon the alkyl migration step. In particular, migration of an alkyl group from a position *cis* to the pyridine moiety to one *trans* to it is extremely unfavorable energetically in the case of ruthenium—a situation which may be exacerbated by the unnaturally short Ru−N(pyridine) bond. For iron, the accessibility of higher multiplicity spin states may serve to alleviate this problem. Further details regarding this unforeseen difference in reactivities will be forthcoming.

Finally, these results may have implications regarding the nature of the active species for the (pybox)Ru-$(C_2H_4)Cl_2$/MAO polymerization system reported recently.[14] Given the quite small amounts of high-molecular-weight polyethylene produced in this system, the question of whether a ruthenium pybox alkyl complex (similar to **3**) is actually responsible for this activity naturally arises.[15]

Experimental Section

All solvents used were dried according to the Grubbs/Dow procedure,[16] and all manipulations were done either in a drybox or under argon or ethylene atmosphere utilizing standard Schlenk and cannula techniques, unless otherwise stated. NMR samples were prepared under an inert atmosphere, utilizing CD_2Cl_2 that was dried over CaH_2 and vacuum-transferred before use. NMR spectra were recorded on a Bruker 400 MHz spectromoter at room temperature, unless otherwise noted. $[Ru(p\text{-cymene})Cl_2]_2$,[7] $[Rh(C_2H_4)_2Cl]_2$,[11] the

(13) Prosenc, M. H.; Brookhart, M. Manuscript in preparation.
(14) Nomura, K.; Warit, S.; Imanishi, Y. *Macromolecules* **1999**, *32*, 4732−4734.
(15) In ref 1a, p 1191, it was mistakenly indicated that "attempts to reproduce this work were unsuccessful". We do not doubt the reproducibility of these results and regret this misstatement. We meant to convey that by analogy with previous transition-metal halide/MAO polymerization systems, the active species is expected to be a cationic Ru pybox alkyl ethylene complex; however, given the inactivity of **3**, it is likely that there is a trace amount of a *different* active species that is responsible for the observed polymerization activity.
(16) Pangborn, A. B.; Giardello, M. A.; Grubbs, R. H.; Rosen, R. K.; Timmers, F. J. *Organometallics* **1996**, *15*, 1518−1520.

ligand **5a**,[3a] and (tmeda)$MgMe_2$[9] were synthesized according to published procedures. $NaB(Ar')_4$ was purchased from Boulder Scientific and used without further purification. Elemental analyses were done by Atlantic Microlabs.

Crystallographic data were collected at −100 °C on a Bruker SMART 1K diffractometer using Mo Kα radiation. Initial cell dimensions and orientation matrices were determined and the frames used to evaluate the quality of the crystals. A full sphere of intensity data were collected with the CCD set to the appropriate maximum 2θ (50−*60*°). The Bruker routine SAINT was used to integrate the frames and produce a set of intensities, which were corrected for absorption effects using SADABS. All subsequent computations were performed using the NRCVAX[17a] suite of programs using scattering factors taken from ref 17b. The structures were solved using direct methods to locate the non-hydrogen atoms. Experimental data are summarized in the Supporting Information.

Synthesis of [(5a)Ru(C_2H_4)Cl_2] (6). A 500 mg amount of [Ru(*p*-cymene)Cl_2]$_2$ (0.816 mmol, 1 equiv) and 618 mg of **5a** (1.67 mmol, 2 equiv) were added to a Schlenk flask connected to a Schlenk line under an ethylene atmosphere. The flask was evacuated and refilled with ethylene, and 25 mL of degassed, absolute ethanol was added. The flask was equipped with a reflux condenser vented to an oil bubbler, purged for 15 min, and then heated to gentle reflux with stirring for 12 h. During this time, the product precipitated as a purple, microcrystalline solid. The reaction mixture was cooled to room temperature and the supernatant removed by cannula filtration. After it was dried overnight in vacuo, the product was extracted from insoluble Ru^0 impurities using CH_2Cl_2. Concentration of the filtrate yielded 770 mg of **6** (83% yield). ^{1}H NMR (CD_2Cl_2): δ 8.163 (ABB′ d, 2H, pyridine H_{meta}), 8.02 (ABB′ t, 1H, pyridine H_{para}), 7.05−7.11 (m, 6H, 2,6-$(CH_3)_2$-C_6H_3), 4.45 (s, 4H, C_2H_4), 2.67 (s, 6H, N=CCH_3), 2.15 (s, 12H, 2,6-$(CH_3)_2$-C_6H_3). ^{13}C{^{1}H} NMR: δ 174.9, 157.2, 148.58, 132.1, 131.1, 128.8, 126.4, 125.3, 82.7, 21.0, 19.0.

Synthesis of [(5a)Ru(C_2H_4)$_2$Cl][B(Ar′)$_4$] (7). Inside a drybox, 500 mg of **6** (0.878 mmol, 1 equiv) and $NaB(Ar')_4$ (0.878 mmol, 1 equiv) were weighed into a Schlenk flask, which was capped with a rubber septum and placed under an ethylene atmosphere on a Schlenk line. CH_2Cl_2 (20 mL) was added via syringe, and the reaction mixture was stirred at room temperature for 2.5 h. The solution was transferred to a separate Schlenk flask via cannula filtration, and the remaining NaCl was washed with 2 × 5 mL of CH_2Cl_2. The combined fractions were dried in vacuo to give a dark brown solid.

Under argon, the solid was dissolved in 10−15 mL of CH_2Cl_2, and an equal volume of pentane was added via syringe. When the mixture was stirred, the product precipitated as a dark red crystalline solid. The flask was cooled to 0 °C in an ice bath to obtain more crystals, and the product was isolated by cannula filtration. Inside the drybox, 1.075 g of **7** was isolated (86% yield). The product is stable under an inert atmosphere at room temperature or below but tends to slowly decompose at higher temperatures. ^{1}H NMR (CD_2Cl_2): δ 8.45 (ABB′ t, 1H, pyridine H_{para}), 8.33 (ABB′ d, 2H pyridine H_{meta}), 7.72 (br m, 8H, B(Ar′)$_4$ H_{ortho}), 7.55 (br s, 4H, B(Ar′)$_4$ H_{para}), 7.07−7.17 (m, 6H, 2,6-$(CH_3)_2$-C_6H_3), 4.38 (s, 4H, C_2H_4), 3.35 (s, 4H, C_2H_4), 2.51 (s, 6H, N=CCH_3), 2.24 (s, 6H, 2,6-$(CH_3)_2$-C_6H_3), 1.82 (s, 6H, 2,6-$(CH_3)_2$-C_6H_3). ^{13}C{^{1}H} NMR: δ 180.3, 162.1 (q, $^1J_{BC}$ = 50 Hz, B(Ar′)$_4$), 160.0, 146.6, 140.2, 135.2 (s, B(Ar′)$_4$), 131.0, 130.5, 130.0, 129.2 (qm, $^2J_{CF}$ = 32 Hz, B(Ar′)$_4$), 128.9, 128.0, 126.8, 125.0 (q, $^1J_{CF}$ = 272 Hz, B(Ar′)$_4$), 117.9 (m, B(Ar′)$_4$), 86.2, 74.7, 20.5, 20.0, 19.0. Anal. Calcd: C, 51.40; H, 3.32; N, 2.95. Found: C, 51.36; H, 3.29; N, 2.94.

Crystals of **7** suitable for X-ray diffraction were grown in a diffusion chamber inside the drybox. Complex **7** (25 mg) was weighed into a vial and dissolved in 1 mL of CH_2Cl_2, which was placed within a larger vial containing 10 mL of pentane. The assembly was sealed, and the crystals were grown over several days at room temperature.

Synthesis of [(5a)Ru(C_2H_4)(CH_3)][B(Ar′)$_4$] (3). Inside the drybox, 500 mg of **7** (0.35 mmol, 1 equiv), 50 mg of (tmeda)-$MgMe_2$ (0.29 mmol), and 320 mg of $NaB(Ar')_4$ (0.36 mmol, 1.03 equiv) were weighed into three separate Schlenk flasks. The flasks were capped with rubber septa and placed under an ethylene atmosphere on a Schlenk line. CH_2Cl_2 (10 mL) was added to both **7** and the (tmeda)$MgMe_2$ via syringe, and the solution of **7** was added to the (tmeda)$MgMe_2$ solution via cannula. The reaction mixture turns dark green upon addition and was stirred for 30 min at room temperature. CH_2Cl_2 (5 mL) was added to the $Na(BAr')_4$ flask, and the reaction mixture was added to the resulting slurry via cannula. After the mixture was stirred for 2 h at room temperature, the solids were removed by cannula filtration and washed with CH_2Cl_2 and the combined filtrate was dried in vacuo to give an oily, dark green-brown residue. The crude product can be purified by two methods.

Method 1. The crude product was dissolved in 4 mL of CH_2Cl_2, and the solution was cooled to −78 °C in a dry ice/acetone bath. A 16 mL amount of pentane was added via syringe, and the mixture was stirred at −78 °C for 20 min to precipitate a dark brown solid. The dark green supernatant is collected by cannula filtration at −78 °C and the solvent removed in vacuo. The product obtained in this manner is a dark green, brittle foam, obtained in 27% yield.

Method 2. The crude product was dissolved in 5 mL of CH_2Cl_2 and loaded via cannula onto a Florisil column (5 cm) under argon. The product was eluted with approximately 50 mL of CH_2Cl_2, and the dark green band was collected in a Schlenk flask. The solvent was removed in vacuo, and the product was isolated as a dark green, brittle foam in 73% yield (350 mg). The product should be stored in a drybox at low temperatures to prevent decomposition. ^{1}H NMR (CD_2Cl_2): δ 8.10 (ABB′ d, 2H, pyridine H_{meta}), 8.01 (ABB′ t, 1H, pyridine H_{para}), 7.71 (br m, 8H, B(Ar′)$_4$ H_{ortho}), 7.55 (br s, 4H, B(Ar′)$_4$ H_{para}), 7.14−7.27 (m, 6H, 2,6-$(CH_3)_2$-C_6H_3), 3.43 (s, 4H, C_2H_4), 2.50 (s, 6H, N=CCH_3), 1.95 (s, 6H, 2,6-$(CH_3)_2$−C_6H_3), 1.38 (s, 6H, 2,6-$(CH_3)_2$-C_6H_3), −1.01 (s, 3H, Ru−CH_3). ^{13}C{^{1}H} NMR: δ 174.6, 162.0 (q, $^1J_{BC}$ = 50 Hz, B(Ar′)$_4$), 155.8, 148.7, 135.1 (s, B(Ar′)$_4$), 133.2, 129.7, 129.1 (qm, $^2J_{CF}$ = 32 Hz, B(Ar′)$_4$), 129.1, 128.2, 127.7, 127.6, 124.9 (q, $^1J_{CF}$ = 272 Hz, B(Ar′)$_4$), 124.8, 117.8 (m, B(Ar′)$_4$), 78.8, 18.9, 18.6, 18.4, −4.8. Anal. Calcd: C, 52.34; H, 3.37; N, 3.05. Found: C, 52.10; H, 3.33; N, 3.17.

Synthesis of [(5a)Ru(C_2H_4)(CH_3)(CO)][B(Ar′)$_4$] (4). Inside the drybox, 50 mg of **3** (0.36 mmol, 1 equiv) was weighed into a Schlenk flask, which was capped with a rubber septum and placed on a Schlenk line under argon. CH_2Cl_2 (5 mL) was added via syringe, and the stopcock to the argon inlet was closed. CO (1 mL, 1.1 equiv) was added via a gastight syringe, and the reaction mixture was stirred for 30 min at room temperature, during which time the solution changed color from dark green to orange. The solvent was removed in vacuo, leaving the product **4** as a brittle foam. ^{1}H NMR (CD_2Cl_2): δ 8.23 (m, 3H, pyridine H_{meta}, H_{para}), 7.72 (br m, 8H, B(Ar′)$_4$ H_{ortho}), 7.55 (br s, 4H, B(Ar′)$_4$ H_{para}), 7.18−7.22 (m, 6H, 2,6-$(CH_3)_2$-C_6H_3), 3.35 (s, 4H, C_2H_4), 2.49 (s, 6H, N=CCH_3), 2.07 (s, 6H, 2,6-$(CH_3)_2$-C_6H_3), 2.02 (s, 6H, 2,6-$(CH_3)_2$-C_6H_3), −0.57 (s, 3H, Ru−CH_3). ^{13}C{^{1}H} NMR: δ 183.7 (CO), 175.5, 162.0 (q, $^1J_{BC}$ = 50 Hz, B(Ar′)$_4$), 154.1, 148.0, 136.9, 135.1 (s, B(Ar′)$_4$), 130.1, 129.7, 129.3, 129.1 (qm, $^2J_{CF}$ = 32 Hz, B(Ar′)$_4$), 128.1, 127.4, 127.3, 124.9 (q, $^1J_{CF}$ = 272 Hz, B(Ar′)$_4$), 117.8 (m, B(Ar′)$_4$), 75.7, 20.0 (Ru-*C*H_3), 19.2, 18.8, 18.4. IR (KBr): ν(CO) 2003 cm^{-1}. Anal. Calcd: C, 52.15; H, 3.30; N, 2.99. Found: C, 52.05; H, 3.33; N, 3.02.

Synthesis of Ligand 5b. A 2 g (12.26 mmol, 1 equiv) amount of 2,6-diacetylpyridine was weighed into a 100 mL round-bottom flask and dissolved in 50 mL of reagent grade 2-propanol. A 6 mL (5.64 g, 28.62 mmol, 2.3 equiv) portion of

(17) (a) Gabe, E. J.; Le Page, Y.; Charland, J.-P.; Lee, F. L.; White, P. S. *J. Appl. Crystallogr.* **1989**, *22*, 384−387. (b) *International Tables for X-ray Crystallography*; Kynoch Press: Birmingham, England, 1974; Vol. IV.

90% 2,6-diisopropylaniline was added by pipet, followed by a catalytic amount (10−20 mg) of camphorsulfonic acid. The flask was equipped with a reflux condenser, and the reaction mixture was heated to a vigorous reflux for 30 h, during which time the product precipitated as a light yellow powder. While it was still warm, the mixture was filtered and the product was collected on a Büchner funnel. (Note: It is important to filter the reaction mixture while it is still warm. When the supernatant cools to room temperature or below, the monoketimine begins to precipitate out of solution. In fact, this product often precipitates as a pure solid out of the filtrate during vacuum filtration.) After drying in vacuo, 5.07 g of **5b** was obtained (86% yield) and used without further purification.

Synthesis of [(5b)RhCl] (8). Inside the drybox, 1 g (2.57 mmol, 1 equiv) of $[Rh(C_2H_4)_2Cl]_2$ and 2.48 g (5.14 mmol, 2 equiv) of **5b** were weighed into a Schlenk flask, which was capped with a rubber septum and placed on a Schlenk line under argon. Toluene (50 mL) was added via syringe, and the reaction mixture was stirred for 24 h at room temperature, during which time the product precipitated as a dark green, microcrystalline solid. The product was isolated by cannula filtration and dried in vacuo. A total of 3.02 g of compound **8** was isolated (95% yield). ^{1}H NMR (CD_2Cl_2): δ 8.51 (t, $^3J_{HH}$ = 8 Hz, 1H, pyridine H_{para}), 7.70 (d, $^3J_{HH}$ = 8 Hz, 2H, pyridine H_{meta}), 7.18−7.31 (m, 6H, 2,6-$(C_3H_7)_2$-C_6H_3), 3.02 (sept, $^3J_{HH}$ = 7 Hz, 4H, ArC$H$$(CH_3)_2$), 1.64 (s, 6H, N=CC$H_3$), 1.12 (d, $^3J_{HH}$ = 7 Hz, 12H, ArCH(CH_3)$_2$), 1.03 (d, $^3J_{HH}$ = 7 Hz, 12H, ArCH-(CH_3)$_2$). ^{13}C{^{1}H} NMR: δ 168.1 (d, $^2J_{RhC}$ = 3 Hz), 156.5 (d, $^2J_{RhC}$ = 3 Hz), 146.2, 140.8, 126.7, 125.3, 124.0, 123.5, 28.5, 23.7, 23.6, 17.9 (d, $^3J_{RhC}$ = 2 Hz). Anal. Calcd: C, 63.92; H, 6.99; N, 6.78. Found: C, 63.74; H, 6.97; N, 6.71.

Synthesis of [(5b)Rh(CH$_3$)(OTf)$_2$] (9). Inside the drybox, 250 mg (0.403 mmol, 1 equiv) of **8** was weighed into a Schlenk flask, which was capped with a rubber septum and placed on a Schlenk line under argon. CH_2Cl_2 (10 mL) was added via syringe, followed by 250 μL (572 mg, 4.03 mmol, 10 equiv) of methyl iodide. The reaction mixture was stirred for 30 min at room temperature, during which time the solution turned from green to dark orange. Under a positive flow of argon, 210 mg (0.806 mmol, 2 equiv) of silver triflate was added as a solid, and the slurry was stirred for 3 h at room temperature, during which time the solution became light orange. The filtrate was collected by cannula filtration, and the remaining solid was extracted with approximately 50 mL of CH_2Cl_2. The combined fractions were evaporated to dryness in vacuo, and the solid obtained was washed with toluene, followed by pentane. After drying, 330 mg of **9** was isolated as a light orange powder (91% yield) and used without further purification. If necessary, **9** can be recrystallized from dichloromethane/pentane. Crystals for X-ray diffraction were grown in a manner similar to that for **7**. ^{1}H NMR (CD_2Cl_2): δ 8.38 (AA′B t, 1H, pyridine H_{para}), 8.09 (AA′B d, 2H, pyridine H_{meta}), 7.18−7.41 (m, 6H, 2,6-$(C_3H_7)_2$-C_6H_3), 3.62 (sept, $^3J_{HH}$ = 7 Hz, 2H, ArC$H$$(CH_3)_2$), 2.54 (s, 6H, N=CC$H_3$), 2.52 (sept, $^3J_{HH}$ = 7 Hz, 2H, ArC$H$$(CH_3)_2$), 2.16 (d, $^2J_{RhH}$ = 2 Hz, 3H, Rh−CH_3), 1.33 (d, $^3J_{HH}$ = 7 Hz, 6H, ArCH(CH_3)$_2$), 1.27 (d, $^3J_{HH}$ = 7 Hz, 6H, ArCH(CH_3)$_2$), 1.21 (d, $^3J_{HH}$ = 7 Hz, 6H, ArCH(CH_3)$_2$), 1.00 (d, $^3J_{HH}$ = 7 Hz, 6H, ArCH-(CH_3)$_2$). ^{19}F NMR: δ −80.4 (s), −81.6 (s). ^{13}C{^{1}H} NMR (triflate carbons not located): δ 181.0, 159.6, 143.4, 140.8, 140.5, 139.9, 129.3, 128.9, 125.8, 125.3, 29.1, 28.9, 26.3, 25.3, 25.0, 21.9, 20.5, 7.4 (d, $^1J_{RhC}$ = 25 Hz, Rh−CH$_3$). Anal. Calcd: C, 48.16; H, 5.16; N, 4.68. Found: C, 48.34; H, 5.19; N, 4.62.

Synthesis of [(5b)Rh(C$_2$H$_4$)][B(Ar′)$_4$] (10). Inside the drybox, 250 mg (0.403 mmol, 1 equiv) of **8** and 357 mg (0.403 mmol, 1 equiv) of NaB(Ar′)$_4$ were weighed into a Schlenk flask, which was capped with a rubber septum and placed on a Schlenk line under an ethylene atmosphere. CH_2Cl_2 (15 mL) was added via syringe, and the reaction mixture was stirred for 4 h at room temperature, during which time the color changed from green to dark orange. The filtrate was collected by cannula filtration, and the remaining NaCl was washed with CH_2Cl_2. After the solvent was removed in vacuo, 530 mg of **10** was obtained as a brown, microcrystalline solid (89% yield). ^{1}H NMR (CD_2Cl_2): δ 8.19 (AA′B t, 1H, pyridine H_{para}), 7.85 (AA′B d, 2H, pyridine H_{meta}), 7.71 (br m, 8H, B(Ar′)$_4$ H_{ortho}), 7.55 (br s, 4H, B(Ar′)$_4$ H_{para}), 7.22−7.41 (m, 6H, 2,6-$(C_3H_7)_2$-C_6H_3), 3.66 (d, $^2J_{RhH}$ = 1 Hz, 4H, Rh−C$_2H_4$), 2.97 (sept, $^3J_{HH}$ = 7 Hz, 4H, ArC$H$$(CH_3)_2$), 2.03 (s, 6H, N=CC$H_3$), 1.27 (d, $^3J_{HH}$ = 7 Hz, 12H, ArCH(CH_3)$_2$), 1.09 ($^3J_{HH}$ = 7 Hz, 12H, ArCH-(CH_3)$_2$). ^{13}C{^{1}H} NMR: δ 174.8 (d, $^2J_{RhC}$ = 2 Hz), 162.0 (q, $^1J_{BC}$ = 50 Hz, B(Ar′)$_4$), 155.6 (d, $^2J_{RhC}$ = 4 Hz), 141.8, 140.2, 139.1, 135.1 (s, B(Ar′)$_4$), 129.1 (qm, $^2J_{CF}$ = 32 Hz, B(Ar′)$_4$), 128.9, 125.7, 125.0, 124.9 (q, $^1J_{CF}$ = 272 Hz, B(Ar′)$_4$), 117.8 (m, B(Ar′)$_4$), 82.8 (d, $^2J_{RhC}$ = 10 Hz, Rh−C_2H_4), 28.7, 24.5, 23.3, 19.4 (d, $^3J_{RhC}$ = 2 Hz). Anal. Calcd: C, 54.52; H, 4.03; N, 2.85. Found: C, 54.44; H, 4.02; N, 2.82.

Synthesis of [(5b)Rh(CH$_3$)(I)][B(Ar′)$_4$] (11). Inside the drybox, 250 mg (0.169 mmol, 1 equiv) of **10** was weighed into a Schlenk flask, which was capped with a rubber septum and placed on a Schlenk line under argon. CH_2Cl_2 (15 mL) was added to dissolve the compound, followed by 25 μL (57 mg, 0.402 mmol, 2.4 equiv) of methyl iodide. The septum was replaced with a glass stopper, and the reaction mixture was heated at 45 °C in a *closed* system for 4 h, during which time the color changed from orange to dark red-pink. The reaction mixture was cooled to room temperature and evaporated to dryness in vacuo. A total of 265 mg of product **11** was isolated as a brittle foam and used without further purification (98% yield). Crystals for X-ray diffraction were grown in a manner similar to that for **7**. ^{1}H NMR (CD_2Cl_2): δ 8.43 (AA′B t, 1H, pyridine H_{para}), 8.12 (AA′B d, 2H, pyridine H_{meta}), 7.73 (br m, 8H, B(Ar′)$_4$ H_{ortho}), 7.56 (br s, 4H, B(Ar′)$_4$ H_{para}), 7.24−7.42 (m, 6H, 2,6-$(C_3H_7)_2$-C_6H_3), 2.43 (s, 6H, N=CCH_3), 2.37 (sept, $^3J_{HH}$ = 7 Hz, 4H, ArC$H$$(CH_3)_2$), 2.16 (d, $^2J_{RhH}$ = 3 Hz, 3H, Rh−CH_3), 1.27 (d, $^3J_{HH}$ = 7 Hz, 6H, ArCH(CH_3)$_2$), 1.24 (d, $^3J_{HH}$ = 7 Hz, 6H, ArCH(CH_3)$_2$), 1.19 (d, $^3J_{HH}$ = 7 Hz, 6H, ArCH(CH_3)$_2$), 1.02 (d, $^3J_{HH}$ = 7 Hz, 6H, ArCH(CH_3)$_2$). ^{13}C{^{1}H} NMR: δ 182.3, 162.0 (q, $^1J_{BC}$ = 50 Hz, B(Ar′)$_4$), 156.7, 143.3, 140.1, 139.2, 139.0, 135.1 (s, B(Ar′)$_4$), 129.8, 129.6, 129.1 (qm, $^2J_{CF}$ = 32 Hz, B(Ar′)$_4$), 124.9 (q, $^1J_{CF}$ = 272 Hz, B(Ar′)$_4$), 124.9, 124.7, 117.8 (m, B(Ar′)$_4$), 32.1, 29.2, 24.9, 24.7, 23.7, 22.8, 20.3, 8.9 (d, $^1J_{RhC}$ = 25 Hz, Rh−CH$_3$). Anal. Calcd: C, 49.86; H, 3.68; N, 2.64. Found: C, 49.87; H, 3.68; N, 2.55.

Generation of [(5b)Rh(CH$_3$)(C$_2$H$_4$)](BF$_4$)$_2$ (12). In a J. Young NMR tube, 10 mg of **11** was dissolved in 0.5 mL of CD_2Cl_2 and an excess of $AgBF_4$ was added (5−7 mg). The tube was immediately frozen in liquid nitrogen and evacuated on a Schlenk line. After it was thawed, the reaction mixture was placed under an ethylene atmosphere. While three distinct species (two major, one minor) are observed initially, only one remains after heating for 1 h at 40 °C, presumed to be **12** due to the disappearance of the B(Ar′)$_4$ signals. ^{1}H NMR (CD_2Cl_2): δ 8.68 (AA′B t, 1H, pyridine H_{para}), 8.43 (AA′B d, 2H, pyridine H_{meta}), 7.47 (AA′B t, 2H, aryl H_{para}), 7.39−7.34 (m, 4H, aryl H_{meta}), 4.29 (d, 4H, $^2J_{RhH}$ = 1 Hz), 3.21 (sept, 2H, $^3J_{HH}$ = 7 Hz, ArC$H$$(CH_3)_2$), 2.67 (s, 6H, N=CC$H_3$), 2.66 (sept, $^3J_{HH}$ = 7 Hz, 2H, ArC$H$$(CH_3)_2$), 1.80 (d, $^2J_{RhH}$ = 2 Hz, 3H, Rh−CH_3), 1.28−1.19 (m, 18H, ArCH(CH_3)$_2$), 1.03 (d, $^3J_{HH}$ = 7 Hz, 6H, ArCH-(CH_3)$_2$).

Acknowledgment. We wish to thank DuPont for funding and Prof. J. L. Templeton for use of laboratory space.

Supporting Information Available: Figures giving the ^{1}H NMR spectrum of compound **12** and X-ray crystal structures of compounds **11** and **13** and tables giving atomic coordinates and isotropic displacement coefficients, anisotropic thermal parameters, bond distances, angles, and packing diagrams for all of the crystal structures. This material is available free of charge via the Internet at http://pubs.acs.org.

OM000674I